Resonance production of diquarks at the CERN LHC

S. Atağ and O. Çakır

Ankara University Department of Physics, Faculty of Sciences, 06100 Tandogan, Ankara, Turkey

S. Sultansoy

Ankara University Department of Physics, Faculty of Sciences, 06100 Tandogan, Ankara, Turkey
and Institute of Physics, Academy of Sciences, Baku, Azerbaijan

Production rates, signatures, and backgrounds are discussed for the first generation scalar diquarks at the CERN LHC using the general, $SU(3)_c \times SU(2)_W \times U(1)_Y$ invariant, effective Lagrangian. It is found that LHC will be able to discover diquarks in the resonance channel with masses up to 3–10 TeV depending on their couplings. [S0556-2821(98)03123-3]

I. INTRODUCTION

The repetition of the three generations of quarks and leptons strongly suggests that they are composite structures made up of more fundamental constituents. They are often called ''preons'' in the literature. The existence of quark and lepton substructure will naturally lead us to expect a rich spectrum of new particles with unusual quantum numbers at high energies such as excited quarks and leptons, diquarks, dileptons, leptoquarks, leptogluons, sextet quarks, octet bosons, etc. Diquarks are those of particles which occur in superstring-inspired E_6 models [1] as well as in composite models [2]. They have integer spin, baryon number $|B| = 2/3$, and lepton number $|L| = 0$.

Searching for composite particles at future collider energies can be classified according to compositeness scale Λ which characterizes the interactions of preons: if $E < \Lambda$ four fermion contact interactions; if $E > \Lambda$ new physics, new particles; if $E \sim \Lambda$ strongly depends on models.

The Collider Detector at Fermilab (CDF) and $D0$ Collaborations [3] at Fermilab recently measured the dijet angular distributions to test QCD and quark compositeness in $\sqrt{s} = 1.8$ TeV $p\bar{p}$ collision assuming the center-of-mass energy of the parton-parton system is smaller than the compositeness scale $\sqrt{\hat{s}} \ll \Lambda$. Their data excluded contact interaction scale below 2 TeV. Then there will be a significant chance of discovering compositeness at the CERN Large Hadron Collider (LHC).

In this work the sensitivity of LHC to diquark production is estimated. We assume that the LHC energy is greater than the compositeness scale Λ if one considers composite diquarks.

II. INTERACTION LAGRANGIAN

There have been a lot of theoretical efforts to construct realistic models for compositeness, but no obviously correct or satisfactory model exists yet. Therefore, within the quark content of the standard model (SM), it is reasonable to construct a model independent, most general, effective $SU(3)_c \times SU(2)_W \times U(1)_Y$ invariant Lagrangian for diquarks:

$$
\begin{aligned}
L = & g_{1L}\bar{q}_L^c i\tau_2 q_L S_1^c + g_{1R}\bar{u}_R^c d_R S_1^c + \tilde{g}_{1R}\bar{d}_R^c d_R \tilde{S}_1^c \\
& + \tilde{g}'_{1R}\bar{u}_R^c u_R \tilde{S}'^c_1 + g_{3L}\bar{q}_L^c i\tau_2 \vec{\tau} q_L . \vec{S}_3^c \\
& + g_2 V_{2\mu}^{cT}\bar{d}_R^c i\tau_2 \gamma^\mu q_L + \tilde{g}_2 \tilde{V}_{2\mu}^{cT}\bar{u}_R^c i\tau_2 \gamma^\mu q_L
\end{aligned}
\tag{1}
$$

where scalar diquarks S_1, $\tilde{S}_1$, $\tilde{S}'_1$ are $SU(2)_W$ singlets and $\vec{S}_3$ is $SU(2)_W$ triplet. V_2 and $\tilde{V}_2$ are vector diquarks which are $SU(2)_W$ doublets. $\psi^c = C\bar{\psi}^T$ is charge conjugated fermion field. Diquarks may transform as antitriplet or sextet under $SU(3)_c$. We assume each SM generation has its own diquarks and couplings to avoid flavor changing neutral currents. In Lagrangian (1) color and generation indices are suppressed for the sake of simplicity. A general classification of the first generation, color $\bar{3}$ diquarks is shown in Table I.

Recent collider limits on the diquark masses come from Tevatron data which exclude $290 < M < 420$ GeV (E_6 diquarks) [4]. There are also constraints on couplings from electroweak precision data from the CERN e^+e^- collider LEP in which the authors give upper bounds on the diquark couplings for their own parametrization taking the diquark mass $M = 100$ GeV [5]. Diquark production at e^+e^- colliders [6], ep colliders [7], and $p\bar{p}$ colliders [8] has also been discussed.

III. DECAY WIDTH AND PRODUCTION CROSS SECTION

For the analysis we will take into account color $\bar{3}$ scalar diquark S_1 which couples to the ud pair as described by the

TABLE I. Quantum numbers of the first generation, color $\bar{3}$ diquarks described by the effective Lagrangian in the text according to $SU(3)_c \times SU(2)_W \times U(1)_Y$ invariance. $Q_{em} = I_3 + Y/2$.

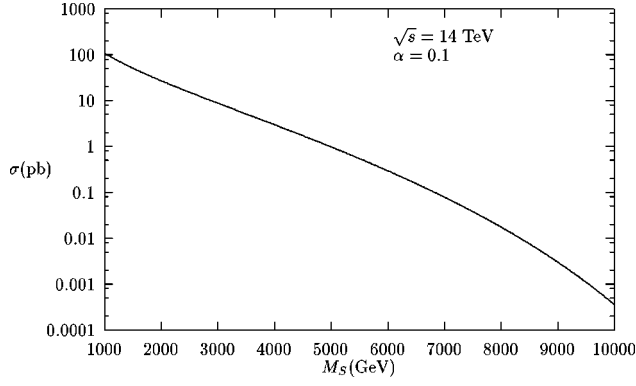| Diquarks	Spin	$SU(3)_c$	$SU(2)_W$	$U(1)_Y$
S_1	0	$\bar{3}$	1	2/3
$\tilde{S}_1$	0	$\bar{3}$	1	−4/3
$\tilde{S}'_1$	0	$\bar{3}$	1	8/3
$\vec{S}_3$	0	$\bar{3}$	3	2/3
V_2	1	$\bar{3}$	2	−1/3
$\tilde{V}_2$	1	$\bar{3}$	2	5/3

FIG. 1. Integrated cross section versus diquark mass for coupling strength $\alpha = 0.1$.

effective Lagrangian (1). The decay width Γ_{S_1} derived from the same Lagrangian is

$$\Gamma_{S_1} = F_c \frac{(g_{1L}^2 + g_{1R}^2)M_s}{16\pi}, \qquad (2)$$

where F_c is the color factor for triplet representation and M_s is the mass of scalar diquark. We will assume $g_{1R} = 0$, and use of the definition $g_{1L}^2 = 4\pi\alpha$ for numerical results:

$$\Gamma_{S_1} = F_c \frac{\alpha M_s}{4} = 25 \ \mathrm{GeV}\left(\frac{F_c M_s}{1 \ \mathrm{TeV}}\right) \quad \text{for} \ \alpha = 0.1 \simeq \alpha_s \qquad (3)$$

$$= 1.8 \ \mathrm{GeV}\left(\frac{F_c M_s}{1 \ \mathrm{TeV}}\right) \quad \text{for} \ \alpha = \alpha_{em}. \qquad (4)$$

In the narrow width approximation the cross section of the s-channel diquark resonance production can be obtained as

$$\sigma(pp \rightarrow S_1 X) = \sum_{ab} \frac{F_c \alpha \pi^2}{s}$$

$$\times \int_{M_s^2/s}^1 \frac{dx}{x} f_a(x, \hat{s}) f_b\left(\frac{M_s^2}{sx}, \hat{s}\right), \qquad (5)$$

where f_a and f_b are quark distribution functions of each proton. Using the quark distribution functions of Ref. [9] the cross section is plotted against the diquark mass in Fig. 1 for LHC energy and $\alpha = 0.1$. If integrated luminosity of LHC 10^5 pb^{-1} is taken into account a high number of events are expected:

$$10^7 \ \text{events} \quad \text{for} \ M_s = 1 \ \text{TeV},$$

$$10^6 \ \text{events} \quad \text{for} \ M_s = 3 \ \text{TeV},$$

$$10^5 \ \text{events} \quad \text{for} \ M_s = 5 \ \text{TeV}.$$

These results show that for much lower coupling constants than α_s, diquark S_1 should be seen at LHC.

TABLE II. QCD backgrounds contributing to j-j final states at the parton level generated by PYTHIA 5.7 with $P_T^{\min} = 100$ GeV.

Process	$\sigma(\text{pb})$
$gg \rightarrow gg$	6.9×10^5
$q_i g \rightarrow q_i g$	6.2×10^5
$q_i q_j \rightarrow q_i q_j$	1.0×10^5
$gg \rightarrow q_k \bar{q}_k$	2.5×10^4
$q_i \bar{q}_i \rightarrow q_k \bar{q}_k$	1.8×10^3
$q_i \bar{q}_i \rightarrow gg$	1.6×10^3

IV. SIGNAL AND BACKGROUND

Resonance production of S_1-type diquarks through the subprocess $u + d \rightarrow S_1 \rightarrow u + d$ will be the promising mechanism to discriminate the signal from QCD backgrounds. The two-jet final state associated with this subprocess is considered as the signal. In addition, there is a contribution from gluon exchange in the t channel which leads to the following cross section:

$$\frac{d\hat{\sigma}}{d\hat{t}}(q_i q_j \rightarrow q_i q_j) = F_c \pi \left[\frac{\alpha^2}{4[(\hat{s} - M_s^2)^2 + M_s^2 \Gamma^2]} \right.$$

$$+ \frac{2\alpha_s^2}{\hat{s}^2} \frac{\hat{s}^2 + \hat{u}^2}{\hat{t}^2} - \frac{\alpha \alpha_s}{\hat{t}}$$

$$\left. \times \frac{\hat{s} - M_s^2}{(\hat{s} - M_s^2)^2 + M_s^2 \Gamma^2} \right]. \qquad (6)$$

At the LHC energy region major QCD processes and their integrated cross sections contributing to two-jet final states as irreducible backgrounds are given in Table II. The cross sections in Table II have been generated by PYTHIA 5.7 [10] at the parton level with a $p_T^{\min} = 100$ GeV.

Standard kinematic relations giving the invariant mass and p_T distributions of two-jet final states are written below for completeness. Let y_1 and y_2 be rapidities for massless final quarks and both are restricted by a cut $-Y \leq y_1, y_2 \leq Y$. Dijet cross section can be written in terms of the transverse momentum p_T possessed by each:

$$\frac{d\sigma}{dp_T}(AB \rightarrow j_1 + j_2 + X) = 4p_T \int_0^{y_{\max}^\star} dy^\star \int_{y_{\min}}^{y_{\max}} dy^b \tau$$

$$\times \left[f_{u/A}(x_u, Q^2) f_{d/B}(x_d, Q^2) \right.$$

$$\times \frac{d\hat{\sigma}}{d\hat{t}}(\hat{s}, \hat{t}, \hat{u}) + f_{d/A}(x_d, Q^2)$$

$$\left. \times f_{u/B}(x_u, Q^2) \frac{d\hat{\sigma}}{d\hat{t}}(\hat{s}, \hat{u}, \hat{t}) \right], \qquad (7)$$
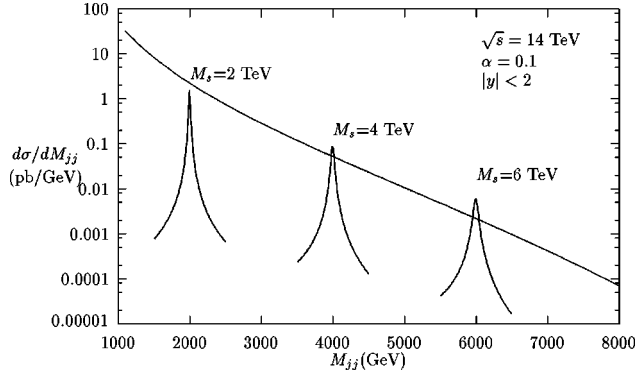
where

FIG. 2. Jet-jet invariant mass distributions for $pp \rightarrow jjX$. Resonance peaks are shown for diquark masses 2, 4, and 6 TeV for comparison with smooth QCD backgrounds.

FIG. 3. p_T distributions for $pp \rightarrow jjX$.

$$y^\star = (y_1 - y_2)/2, \quad y^b = (y_1 + y_2)/2, \quad \tau = \frac{4p_T^2}{s} \cosh^2 y^\star, \tag{8}$$

$$y^\star_{\max} = \log \left[\left(\frac{s}{4p_T^2} \right)^{1/2} + \left(\frac{s}{4p_T^2} - 1 \right)^{1/2} \right], \tag{9}$$

$$y_{\min} = \max \left(-Y, \frac{1}{2} \log \tau \right), \quad y_{\max} = \min \left(Y, -\frac{1}{2} \log \tau \right), \tag{10}$$

$$x_u = \sqrt{\tau} e^{y^b}, \quad x_d = \sqrt{\tau} e^{-y^b}, \tag{11}$$

$$\hat{s} = x_u x_d s, \quad \hat{t} = -x_u p_T \sqrt{s} e^{-y_1}, \quad \hat{u} = -x_d p_T \sqrt{s} e^{y_1}. \tag{12}$$
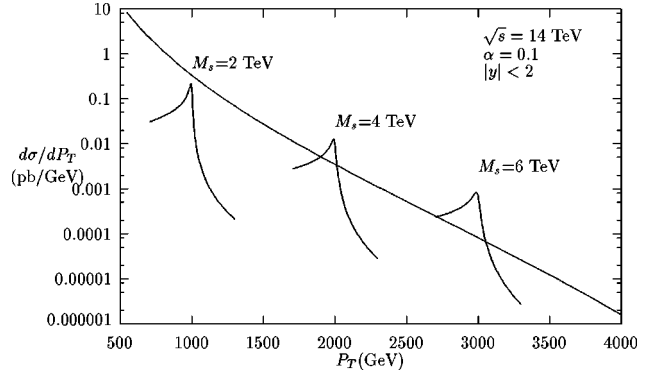
The cross section as a function of the dijet invariant mass M_{jj} is given by

$$\frac{d\sigma}{dM_{jj}} = \frac{M_{jj}^3}{2s} \int_{-Y}^{Y} dy_2 \int_{y_1^{\min}}^{y_1^{\max}} dy_1 \frac{1}{\cosh^2 y^\star}$$

$$\times \left[f_{u/A}(x_u, Q^2) f_{d/B}(x_d, Q^2) \frac{d\hat{\sigma}}{d\hat{t}}(\hat{s}, \hat{t}, \hat{u}) \right.$$

$$\left. + f_{d/A}(x_d, Q^2) f_{u/B}(x_u, Q^2) \frac{d\hat{\sigma}}{d\hat{t}}(\hat{s}, \hat{u}, \hat{t}) \right] \tag{13}$$

with

$$y_1^{\min} = \max(-Y, \log \tau - y_2), \quad y_1^{\max} = \min(Y, -\log \tau - y_2),$$

$$\tau = M_{jj}^2/s. \tag{14}$$

TABLE III. Observability of the diquark signal for integrated luminosity 10^5 pb^{-1} and diquark coupling strength $\alpha = 0.01$.

Mass (TeV)	1	2	3	4	5	7	8
$|y| < 3$							
Signal	1.7×10^6	4.2×10^5	1.4×10^5	4.7×10^4	1.5×10^4	1.2×10^3	2.8×10^2
Backgd.	3.7×10^9	2.9×10^8	5.2×10^7	1.2×10^7	2.9×10^6	1.6×10^5	2.9×10^4
$S/\sqrt{B}$	27.3	24.9	19.2	13.6	9.0	3.2	1.6
$|y| < 2$							
Signal	1.3×10^6	3.7×10^5	1.3×10^5	4.4×10^4	1.5×10^4	1.2×10^3	2.6×10^2
Backgd.	3.6×10^8	2.9×10^7	5.3×10^6	1.2×10^6	3.0×10^5	1.6×10^4	3.1×10^3
$S/\sqrt{B}$	68.9	69.6	55.5	39.9	26.5	9.4	4.8
$|y| < 1$							
Signal	5.1×10^5	1.8×10^5	7.0×10^4	2.7×10^4	9.6×10^3	8.5×10^2	1.9×10^2
Backgd.	3.2×10^7	2.7×10^6	5.0×10^5	1.2×10^5	3.0×10^4	1.6×10^3	3.0×10^2
$S/\sqrt{B}$	90.0	108.7	99.0	78.2	55.4	21.1	11.1
$|y| < 0.5$							
Signal	1.4×10^5	5.4×10^4	2.3×10^4	9.6×10^3	3.7×10^3	3.9×10^2	95.9
Backgd.	6.1×10^6	5.3×10^5	1.0×10^5	2.6×10^4	6.9×10^3	4.1×10^2	79.1
$S/\sqrt{B}$	58.6	73.8	70.7	59.1	44.8	19.4	10.8

TABLE IV. The same as the Table III for $\alpha = 0.1$.

Mass (TeV)	1	2	3	4	5	7	9
$|y|<3$							
Signal	1.6×10^7	4.2×10^6	1.4×10^6	4.7×10^5	1.5×10^5	1.2×10^4	4.8×10^2
Backgd.	3.7×10^9	2.9×10^8	5.2×10^7	1.2×10^7	2.9×10^6	1.6×10^5	4.4×10^3
$S/\sqrt{B}$	272.6	248.8	192.4	136.4	90.2	31.5	7.3
$|y|<2$							
Signal	1.3×10^7	3.7×10^6	1.3×10^6	4.4×10^5	1.5×10^5	1.2×10^4	4.6×10^2
Backgd.	3.6×10^8	2.9×10^7	5.3×10^6	1.2×10^6	3.0×10^5	1.6×10^4	4.5×10^2
$S/\sqrt{B}$	689.4	685.6	554.8	398.6	265.4	93.6	21.6
$|y|<1$							
Signal	5.1×10^6	1.8×10^6	7×10^5	2.7×10^5	9.6×10^4	8.5×10^3	3.4×10^2
Backgd.	3.2×10^7	2.7×10^6	5.0×10^5	1.2×10^5	3.0×10^4	1.6×10^3	44.9
$S/\sqrt{B}$	898.8	1087.1	992.1	782.1	554.5	211.2	51.1
$|y|<0.5$							
Signal	1.4×10^6	5.4×10^5	2.3×10^5	9.5×10^4	3.7×10^4	3.9×10^3	1.8×10^2
Backgd.	6.1×10^6	5.3×10^5	1.0×10^5	2.6×10^4	6.9×10^3	4.1×10^2	12.0
$S/\sqrt{B}$	586.1	737.9	706.7	590.8	447.7	194.0	51.6

Figures 2 and 3 shows jet-jet invariant mass and p_T distribution for the process $pp \to S_1 \to jjX$ together with estimates of the QCD backgrounds at LHC energy $\sqrt{s} = 14$ TeV. For scalar diquark masses $M_s = 2, 4, 6$ TeV and $\alpha = 0.1$ signal peaks and backgrounds are plotted for comparison.

In order to obtain observability of diquarks at LHC we have calculated signal and background event estimations for integrated LHC luminosity $10^5 pb^{-1}$. To arrive at realistic estimates we take into account the finite-energy resolution of the LHC-ATLAS hadronic calorimeter [11]

$$\frac{\delta E}{E} = \frac{50\%}{\sqrt{E}} + 3\% \qquad (15)$$

for hadronic jets and for $|y|<3$. From the dijet invariant mass definition for massless jets

$$M_{jj} = \sqrt{2E_{j_1}E_{j_2}(1 - \cos\theta_{12})}, \qquad (16)$$

it is easy to obtain jet-jet invariant mass resolution as

$$\frac{\delta m}{m} = \frac{1}{2}\sqrt{\left(\frac{\delta E_{j_1}}{E_{j_1}}\right)^2 + \left(\frac{\delta E_{j_2}}{E_{j_2}}\right)^2 + \left(\cot\frac{\theta_{12}}{2}\right)^2(\delta\theta_{12})^2}, \qquad (17)$$

where E_{j_1}, E_{j_2} are the jet energies and θ_{12} is the jet-jet opening angle. We consider only the errors on the jet energies, as these are much larger than the errors on the angle measurements. Assuming that the errors on both energies are close to each other on the average, $\delta m/m$ can be taken as $\delta E/\sqrt{2}E$. For background estimations we integrate the in-

variant mass distribution of the background over twice the diquark width Γ or the invariant mass resolution δm depending on their magnitude

$$\sigma_{bg} \approx \int_{M-\Delta M}^{M+\Delta M} dM_{jj} \left(\frac{d\sigma}{dM_{jj}}\right)_{bg}, \qquad (18)$$

where

$$\Delta M = \max(\Gamma, \delta m). \qquad (19)$$

For signal estimation the width $\mp\Gamma$ of diquark has been used as the integration limits.

The expected events and significancy of diquark signals at LHC are given in Tables III and IV for couplings $\alpha = 0.01$ and $\alpha = 0.1$. As can be seen from these tables discovery limits depend on the y cut chosen. Furthermore, the lower rapidity region improves the signal-to-noise ratio. Achievable mass limits for different coupling values are shown in Table V which are satisfying the following two criteria per one working year: At least 100 signal events within cuts, $s/\sqrt{B}>5$. For the $\alpha=0.1$ value in Table V it is possible to

TABLE V. Achievable diquark mass limits for different diquark-quark-quark couplings in the framework of discovery criteria given in the text. $|y|<2$.

α	Mass (TeV)	Signal	Backgd.	$S/\sqrt{B}$
0.1	9.7	109	98	17
0.01	7.9	312	3646	5.2
0.001	3.3	9.3×10^3	3.3×10^6	5.1

reach higher mass values than 10 TeV with $S/\sqrt{B} > 5$ if the period of 100 signal events is extended to two or more working years.

In conclusion, diquarks are produced with a large cross section in resonance channel at LHC. From Tables III and IV we see that the signal separation from Standard model backgrounds is highly promising. Diquarks with masses up to almost 8 TeV can be discovered for coupling strengths $\alpha = 0.01$ with realistic probability. For lower couplings such as 1×10^{-3} it is possible to probe masses around 3 TeV. If diquarks with lower coupling strengths exist we will need a high-resolution calorimeter for the experimental identification of hadronic jets. Certainly, a careful Monte Carlo reconstruction including whole detector parameters should be done in order to make a firm decision.

[1] J. L. Hewett and T. G. Rizzo, Phys. Rep. **183**, 193 (1989).

[2] B. Schrempp, *Talk at the 23rd International Conference on High Energy Physics* (Berkeley, 1986), MPI-PAE/PTh 72/86; for a review, see W. Buchmüller, Acta Phys. Austriaca, Suppl. **27**, 517 (1985).

[3] CDF Collaboration, F. Abe *et al.*, Phys. Rev. Lett. **77**, 5336 (1996); DO Collaboration, B. Abbott *et al.*, *ibid.* **80**, 666 (1998).

[4] T. Dorigo, FERMILAB-Conf-97/281-E (1997).

[5] G. Bhattacharya, D. Choudhury, and K. Sridhar, CERN Report No. CERN-TH /95-89 (1995).

[6] D. Schaile and P. M. Zerwas, *Proceedings of the Workshop on Physics at Future Accelerators*, CERN yellow report 87-07, Vol. II, p. 251 (1987).

[7] T. G. Rizzo, Z. Phys. C **43**, 223 (1989).

[8] V. D. Angelopoulos *et al.*, Nucl. Phys. **B292**, 59 (1987).

[9] A. D. Martin, W. J. Stirling, and R. G. Roberts, Phys. Lett. B **354**, 155 (1995).

[10] T. Sjöstrand, Comput. Phys. Commun. **82**, 74 (1994).

[11] ATLAS Technical Proposal, CERN, Geneva, 1994.